Dispersion analysis in wave propagation using parametrized mimetic finite differences.

Author: Miguel Ferrer Àvila.
*Facultat de Física, Universitat de Barcelona, Diagonal 645, 08028 Barcelona, Spain.**

Advisor: Pilar Queralt Capdevila.
Co-Advisor: Josep de la Puente (BSC).

Abstract: Wave propagation simulations using numerical methods are subject to dispersion errors due to the discrete nature of the differentiation operator. To minimize the effects of dispersion, high-order operators are preferred to solve the wave propagation model. The mimetic finite-difference method is a family of fourth-order finite-difference operators which can be constructed by varying a set of six free parameters. In this work, I explore the effect of varying these parameters on the dispersion of elastic waves, in search of the optimal set of values to minimize this anomaly in a one-dimensional problem.

I. INTRODUCTION

A challenge that often arises in physics problems, from quantum mechanics to signal transmission, is solving a specific form of the wave equation. In particular, simulating the propagation of seismic waves in heterogeneous, three-dimensional media is at the core of many geophysical exploration problems. Seismic surveys obtain data of the underground structures by measuring the response of the ground to disturbances, in the form of elastic waves that propagate through the Earth's crust and its surface. The waves are scattered (refracted and reflected back to the surface) when there are changes in the properties of the medium in which they travel. Arrays of seismographs can measure the magnitude of the reflected waves and their arrival times. Using this data, geophysicists can generate images of the subsurface. In order to obtain high-resolution images that better represent the real geology, it is important that the wave propagation is modeled as accurately as possible.

The complexity of the simulation prevents us from finding an analytical solution to the wave equation, and therefore we must resort to approximating numerical solutions. The accuracy of the approximated solution is determined by several factors, including how close the simulation represents the underlying physical problem, and the order of the numerical method used. Higher-order methods produce more accurate results, with reduced dispersion compared to their lower-order counterparts, but in return have a greater cost in terms of computing resources.

Nowadays, the most popular numerical method used to model seismic waves is the Finite-Difference (FD) method, due to its simplicity and its straightforward implementation. Furthermore, the FD operator can be designed for a specific order of accuracy, and can be very efficient, as it is relatively easy to optimize compared to other methods. However, this method presents some disadvantages; high-order FD operators struggle to include accurate solutions for boundary conditions, as well as to deal with irregularly shaped domains—for instance, when including surfaces with topographic features.

Seismic simulations typically incorporate a free surface condition, on top of the domain, to simulate the tractionless interface between ground and air. The free surface is a Dirichlet boundary condition, in which the wave does not exert traction in the vertical direction, and it must be accurately represented in the propagation in order to simulate realistic surface waves (such as Rayleigh waves).

In order to tackle the free-surface condition, we use a family of operators called the Mimetic FD (MFD) operators. These operators preserve the Gauss divergence theorem using lateral stencils to approximate wavefield fluxes at boundaries. The MFD method provides two operators that can be constructed with any accuracy order, from a set of three free parameters for each operator.

In this work, I study the effect of varying the parameters when constructing the MFD operators, analyzing the impact that different operators have on the dispersion of elastic waves. I look for optimal parameters that minimize dispersion in a one-dimensional array, and compare several MFD and standard FD operators to find the method with the lowest dispersion.

II. MIMETIC FINITE DIFFERENCE OPERATORS FOR ELASTIC WAVES

The elastic equation of motion is usually formulated as a pair of coupled differential equations thus,

$$\begin{aligned} \rho\frac{\partial v_i}{\partial t} &= \partial_j\sigma_{ij} + F_i(t) \\ \frac{\partial \sigma_{ij}}{\partial t} &= C_{ijkl}\,\frac{1}{2}(\partial_k v_l + \partial_l v_k), \end{aligned} \tag{1}$$

where ρ is the density of the medium, v_i represents the velocity component in the i direction, ∂_i is the derivative in the i direction, σ_{ij} represents the stress tensor in index notation, $F_i(t)$ is the source force component, and C_{ijkl} is the fourth-order stiffness tensor. If the interface

*Electronic address: miguel.ferrer@bsc.es

between the ground and the air is the top xy-plane of the domain, then the Dirichlet free-surface condition is given by $\sigma_{zz}|_{z=0} = 0$. We can reduce the number of equations by limiting the problem to a one-dimensional system, and simplify them by considering an isotropic medium. The equations become

$$\begin{aligned} \rho \frac{\partial v_x}{\partial t} &= \frac{\partial \sigma_{xx}}{\partial x} + F_x(t) \\ \frac{\partial \sigma_{xx}}{\partial t} &= (\lambda + 2\mu) \frac{\partial v_x}{\partial x}, \end{aligned} \tag{2}$$

where λ and μ are the Lamé parameters, which depend on the material properties of the propagating media.

To solve the system numerically, we approximate the spatial derivatives using the fourth-order FD method, following [1]. To do so, we discretize the propagation domain in the spatial dimension using a staggered-grid approach, in which two grids (one with stress nodes and one with velocity nodes) are interleaved, as seen in Figure 1.

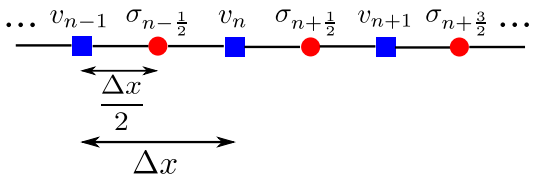

Figure 1: The staggered-grid scheme in one dimension.

With this scheme, the spatial derivative becomes a discrete stencil operator. The expression for the fourth-order stencil is as follows

$$\partial_x f_k \approx \frac{c_1 \left(f_{k+\frac{1}{2}} - f_{k-\frac{1}{2}}\right) + c_2 \left(f_{k+\frac{3}{2}} - f_{k-\frac{3}{2}}\right)}{\Delta x} = S_x[f_k] \tag{3}$$

where S is the *centered* FD operator, f_k represents the variable to differentiate at node k, Δx is the spatial discretization, and c_1, c_2 are the operator coefficients, with values of $c_1 = \frac{9}{8}$ and $c_2 = \frac{1}{24}$ for the fourth-order operator on staggered grids [1][2]. It is referred to as *centered* stencil because node values on both sides of the node k are necessary to compute the derivative at node k.

Due to the lack of stress and velocity nodes beyond the boundaries of our domain, the centered stencil operator can not compute derivatives close to or at the grid boundary. To update nodes at those locations, we use a *lateral* stencil operator. However, regular FD operators become less precise when lacking node values on each side of the node to differentiate. To preserve the order of accuracy of our operator, we employ the MFD operators following the work of [3].

The MFD operators on staggered grids require one extra node to compute the derivative at the boundary. This extra node shares its location on the grid with the boundary node. In our case, we model the domain so that it has two free-surface conditions, one at each boundary of the one-dimensional grid. The resulting scheme is illustrated in Figure 2.

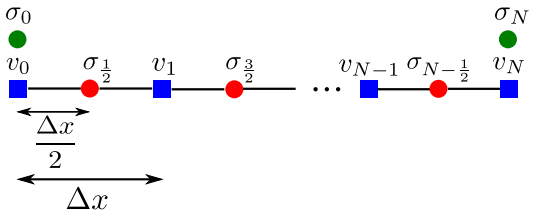

Figure 2: The boundaries of our staggered grid with the mimetic extra nodes in green.

The derivatives of the stress nodes are computed using the *Mimetic Gradient* operator, G, while the derivatives of the velocity nodes are computed using the *Mimetic Divergence* operator, D [4]:

$$\frac{\partial \sigma_{xx}}{\partial x} \approx G[\sigma_{xx}] \qquad \frac{\partial v_x}{\partial x} \approx D[v_x]. \tag{4}$$

There are three degrees of freedom when constructing the operators, as their coefficients depend on three parameters each: α_G, β_G and γ_G for G; and α_D, β_D and γ_D for D, as shown in [3]. The operators hold the coefficients that compute all the first derivatives of the grid; however, the mimetic coefficients are only particular to the derivatives computed close to the boundaries. As the operator moves to the interior points of the grid, the stencil coefficients match those of the standard FD operator discussed before. Thus, the D and G operators have a maximum mimetic bandwidth. For the fourth-order MFD operators, the bandwidth is the first four points of the grid, although the α, β, and γ parameters can be chosen so as to make the operator more compact—that is, having a smaller bandwidth.

For time integration, we use the second-order leapfrog method so that we can recover the stress and velocity components. This explicit method keeps the velocity and stress nodes updated with their values computed half a time step apart, thus resulting in the following system,

$$\begin{aligned} \rho \frac{\partial v_x}{\partial t} &\approx \rho \frac{v_x^{m+1} - v_x^m}{\Delta t} \\ v_x^{m+1} &\approx v_x^m + \frac{\Delta t}{\rho} G[\sigma_{xx}^m], \end{aligned} \tag{5}$$

from equations (2), (4), where Δt represents the time discretization, and I have omitted the force term. Similarly, to update stresses,

$$\sigma_{xx}^{m+\frac{3}{2}} \approx \sigma_{xx}^{m+\frac{1}{2}} + \Delta t\, (\lambda + 2\mu)\, D[v_x^{m+1}]. \tag{6}$$

There are other methods available to integrate in the temporal dimension, but I will not delve into them. Suffice it to say that methods with higher order have a significant impact in the dispersion of the elastic wave, but this accuracy comes at a cost, as most methods require storing information at extra points in time, which greatly increases the memory cost of the simulation [8].

III. OPTIMIZING THE MIMETIC OPERATORS

In order to analyze the behavior of the mimetic operators, I construct a test consisting of a one-dimensional staggered grid with free-surface boundary conditions at both ends. The domain is considered homogeneous in terms of material properties. I initialize the stress nodes of the grid with a Ricker wavelet, centered within the domain. The wave propagates both ways in the x-direction, until it reaches the free surface and is reflected back toward the center. For an ideal, analytical solution, the superposition of the two reflected wavelets should be an exact reconstruction of the initial pulse, as there are no dissipative effects—such as viscoelasticity—in the test.

I use two main criteria for assessing the quality of our operator: the misfit function and the maximum Courant number, C_{max}, allowed by the operator.

The misfit function measures the relative discrepancy between the reconstructed wave and the original source, in phase and envelope terms; therefore, operators that are less dispersive will produce results with lower phase misfit than their more dispersive counterparts, while operators that are less dissipative will produce results with lower envelope misfit. In order to find the optimal parameters to generate less dispersive MFD operators, I have developed a C code that scans the solution space looking for operators that minimize the misfit function. The algorithm can be tuned for a specific size of the parameter domain to explore,

$$\mathcal{P} = [p_{min}^{\alpha_G}, p_{max}^{\alpha_G}] \times [p_{min}^{\alpha_D}, p_{max}^{\alpha_D}] \times \ldots \times [p_{min}^{\gamma_D}, p_{max}^{\gamma_D}], \quad (7)$$

with each p_{min}, p_{max} representing the domain limits for each of the six parameters. The parameter discretization can then be computed as,

$$\begin{aligned} dp^k &= \frac{p_{max}^k - p_{min}^k}{N} \qquad k \in \{\alpha_G, \beta_G, \gamma_G, \alpha_D \ldots\} \\ p_i^k &= p_{min}^k + i \cdot dp^k \qquad i \in \{0, 1, \ldots, N-1, N\}, \end{aligned} \quad (8)$$

and the discretized parameter domain to explore is

$$\mathcal{P}' = \{(p_{i_1}^{\alpha_G}, p_{i_2}^{\beta_G}, p_{i_3}^{\gamma_G}, p_{i_4}^{\alpha_D}, p_{i_5}^{\beta_D}, p_{i_6}^{\gamma_D})\}. \quad (9)$$

Due to the nature of the optimization problem, the number of solutions to test can be very large: N^6. By choosing $p_{min} = -1$, $p_{max} = 1$ and $N = 20$, which yields a coarse discretization $dp = 0.1$, we need to run the test 64 million times, taking more than 40 days to compute. In order to test a finer discretization, we can progressively reduce the range of the parameter domain, adapting p_{min}^k and p_{max}^k to leave out regions which yield more dispersive operators. I have parallelized the program using the *Message Passing Interface* (MPI) standard so that it executes in multiple computing nodes, each running tests on non-overlapping regions of the parameter domain. As a consequence, I can explore each region of the parameter domain in hours instead of days.

The maximum Courant number of an operator, C_{max}, quantifies the stability limit of the operator in terms of the FD method and the particular grid we are using to propagate the wave. The Courant-Friedrichs-Lewy (CFL) condition states that, for a simulation to be stable, it is necessary that C, as determined by the grid parameters, is lower than the maximum Courant number allowed by the operator, C_{max},

$$C \;=\; \frac{v_p\, \Delta t}{\Delta x} \leq C_{max}, \quad (10)$$

where v_p is the maximum velocity of the wave. Thus, for a constant wave velocity and discretization of our problem, operators with greater Courant numbers require less iterations of our simulation method, as greater time steps can be used.

The CFL condition is a specific form of the Lax equivalence theorem [5]. Let us consider the leapfrog scheme presented in Equations (5) and (6) in its simplified form

$$u^{n+1} \;=\; Su^n, \quad (11)$$

where u is the array representing the grid to update, and S is the FD operator. The theorem states that S is stable (and therefore, the method converges) if for an arbitrary initial condition u^0, operator S is upper bounded; that is, there is an upper bound constant K such that,

$$||S^n|| \;\leq\; K, \quad (12)$$

with $K \geq 1$. A necessary and sufficient condition to satisfy the Lax equivalence theorem involves the spectral radius of the operator S. The spectral radius of an operator is the maximum magnitude of its eigenvalues. In order for the FD operator to satisfy equation (12), and therefore be stable, it must have a spectral radius less than or equal to 1. Therefore, C_{max} can be computed as the spectral radius of the operator, and $C_{max} \leq 1$ [6].

IV. RESULTS

I set the test case to have a fixed P-wave velocity, $v_p = 3000$ m/s, a fixed spatial discretization $\Delta x = 10$ m, and a fixed Courant number $C = 0.5$; this sets the temporal discretization to $\Delta t = 1.67$ ms. I propagate the wave enough time so that it reflects against the free-surface boundaries ten times. By exploring the parameter space using the misfit function and the CFL criteria as stated above, I obtain several mimetic operators worthy of consideration. I compare their characteristics to other already established FD operators, and summarize them in Table I.

The *Compact* mimetic operator is presented in [3] as a MFD operator with the smallest mimetic bandwith

Operator	Parameters (α_G, β_G, γ_G, α_D, β_D, γ_D)	C_{max}
Compact	$(0,\ 0,\ \frac{-1}{24},\ 0,\ 0,\ \frac{-1}{24})$	0.81
Taylor	Not applicable (non-mimetic)	0.81
Adjoint	$(\frac{142}{3715},\ \frac{-624}{15839},\ \frac{-21}{23707},\ \frac{488}{10121},\ \frac{-367}{7075},\ \frac{-167}{7167})$	0.85
Alpha	$(\frac{-799}{999},\ 0,\ \frac{-21}{23707},\ \frac{233}{999},\ 0,\ \frac{-1}{24})$	0.50
Beta	$(0,\ \frac{-699}{999},\ \frac{-1}{24},\ 0,\ \frac{-227}{999},\ \frac{-1}{24})$	0.64
Optimal	$(\frac{5}{9},\ \frac{-259}{999},\ \frac{-629}{999},\ \frac{2}{9},\ \frac{-1}{9},\ \frac{-370}{999})$	0.68

Table I: Operators, parameters to construct them and their maximum Courant number.

possible—one point in the D operator and two points in the G operator, with fourth-order accuracy. The *Taylor* operator is a regular lateral FD operator, constructed according to [2]. The *Adjoint* operator is a quasi-adjoint MFD operator presented in [7], which approximates the mimetic operators to their negative adjoint form, such that $G \approx -D^T$. A benefit of using the quasi-adjoint operator is its increased numerical stability for the second-order leapfrog integration method, as this operator has a higher maximum Courant number than the *Compact* counterpart. The *Alpha* operator is obtained by using our algorithm on the α_G and α_D parameters, while keeping the rest with the same values as the *Compact* operator. We can obtain the *Beta* operator by optimizing for the β_G and β_D parameters in the same manner. Finally, the *Optimal* operator is obtained optimizing for all the parameters concurrently.

Operator	Envelope misfit	Phase misfit
Compact	42.9%	14.9%
Taylor	43.6%	14.9%
Adjoint	42.8%	14.9%
Alpha	8.1%	2.0%
Beta	17.0%	2.8%
Optimal	5.7%	1.1%

Table II: Operators and the envelope and phase misfit results after propagating a wave in our test case.

Considering the Courant number of each operator, the MFD operators I obtain using our algorithm are more restrictive of the problem definition in order to remain stable. The *Optimal* operator has a C_{max} that is 16% smaller than the more stable *Compact* operator. For a given v_p and Δx, the Δt of the *Optimal* operator would have to be 84% smaller, which results in an increase in the total number of iterations that the simulator has to compute, to 1.19× the original, that is, 19% more iterations.

However, when considering the accuracy of the results, our operators outperform the rest. Table II illustrates the effect that each operator has in reducing the dispersion on the test case. Figure 3 showcases a sample wave reconstruction, with different wave profiles depending on the operator used. The impact on dispersion is noticeable in the wave reconstruction, especially for the *Compact* operator.

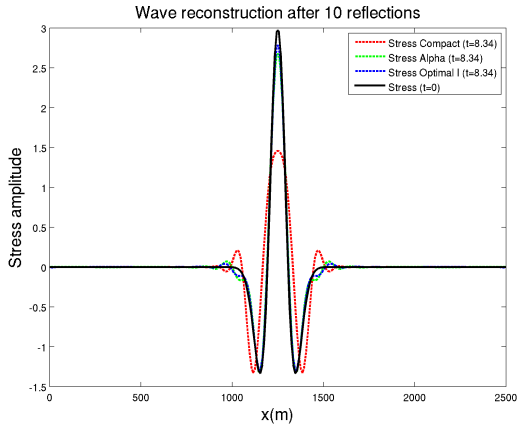

Figure 3: Reconstruction of the initial wave (stress component) depending on the operator used. The *Taylor* and *Adjoint* operator produce results almost indistinguishable to *Compact*, so they are omitted from figures for clarity.

The effects of dispersion on both wave envelope and wave phase are minimized using our operator, as Figures 4 and 5 illustrate. For ten reflections, the *Optimal* operator exhibits a 87% decrease for the envelope misfit and a 92% for the phase misfit. This increased accuracy is preserved as the number of reflections grows, with an 80% and 84% reduction in the envelope and phase misfit respectively, at twenty reflections.

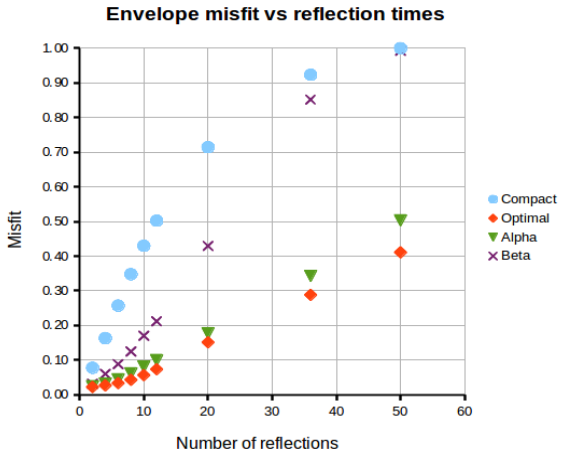

Figure 4: As the number of reflections against the free surface increases, so does the misfit due to dissipation. Our operator *Optimal* is less dissipative.

Figure 6 highlights the increased rate of convergence of the *Optimal* operator to the analytical solution as the number of nodes in the grid increases and the spatial discretization decreases. Fourth-order operators require at least six points per wavelength (PPW) to model the wave propagation [1].

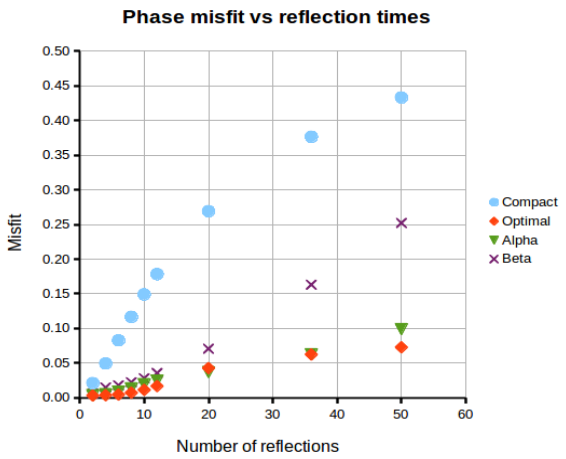

Figure 5: Simlarly, the phase misfit also increases with the number of reflections due to dispersion. The *Optimal* operator is less dispersive and outperforms the other operators in phase reconstruction.

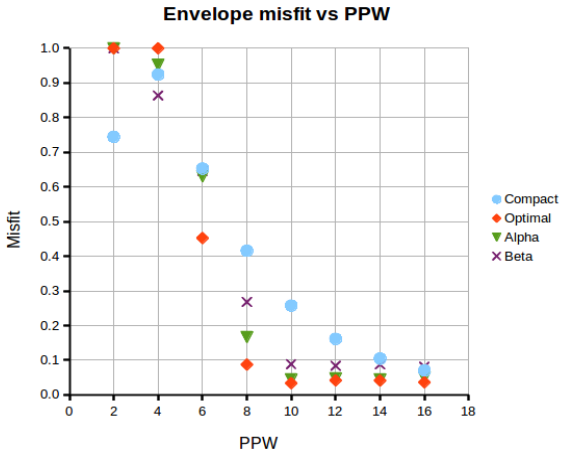

Figure 6: Convergence of the operators as the number of grid nodes (PPW) increases, and spatial discretization decreases.

V. CONCLUSIONS

The mimetic operators are a parametric set of FD operators that allow us to obtain solutions for the elastic wave propagation that satisfy the conservation laws with high order of accuracy for FD problems with Dirichlet boundary conditions.

These operators can be constructed by varying six free parameters. I develop a parallel scanning algorithm to perform an optimization process, and find a set of parameters to build an MFD operator that minimizes dispersion on waves that propagate in a one-dimensional medium with free-surface condition on its sides.

The resulting *Optimal* mimetic operator outperforms other mimetic and non-mimetic operators in reducing the dispersion across the range of valid points-per-wavelength. This increase in accuracy has no cost in terms of the computing resources, as it consists of substituting the original mimetic operator coefficients with those of the *Optimal* operator. However, there is a trade-off, as the operator is less stable for problems with a higher Courant number. Regardless, the stability limits of this operator are well included within the range of typical geophysics applications.

Acknowledgments

I would like to thank my advisors, Dr. Pilar Queralt and Dr. Josep de la Puente, for their guidance, support and suggestions to improve this work. I would also like to thank Dr. Otilio Rojas for helping me navigate the theoretical foundation on which this work is built. Finally, I would like to thank my family, for always being there for me.

[1] Levander, A. R. "Fourth-order finite-difference P-SV seismograms". Geophysics **53**: 1425-1436 (1988).
[2] Fornberg, B. "Generation of Finite Difference Formulas on Arbitrarily Spaced Grids". Mathematics of Computation **51**: 699-706 (1988).
[3] Castillo, J.E., Hyman, J.M., Shashkov, M. and Steinberg, S. "Fourth and Sixth-Order Conservative Finite-Difference Approximations of the Divergence and Gradient". Applied Numerical Mathematics **37**: 171-187 (2001).
[4] de la Puente, J., Ferrer, M., Hanzich, M., Castillo, J.E. and Cela, J.M. "Mimetic seismic wave modeling including topography on deformed staggered grids". Geophysics **79**: T125-T141 (2014).
[5] Lloyd N. Trefethen "Finite Difference and Spectral Methods for Ordinary and Partial Differential Equations". Unpublished text (1996). Available at `http://people.maths.ox.ac.uk/trefethen/pdetext.html`
[6] Zingg, D.W. and Lederle, M. "On Linear Stability Analysis of High-Order Finite-Difference Methods". 17th AIAA Computational Fluid Dynamics Conference (2005).
[7] Córdova, L., Rojas, O., Otero, B. and Castillo, J.E. "Compact Finite Difference Schemes for the Acoustic Wave Equation". 78th EAGE Conference and Exhibition (2016).
[8] P. Moczo, J. Kristek *The Finite-Difference Modelling of Earthquake Motions: Waves and Ruptures*, (Cambridge University Press, 2014, 1st. ed.).